

**NANO EXPRESS**

**Open Access**

# Coherent anti-Stokes Raman scattering enhancement of thymine adsorbed on graphene oxide

Galyna Dovbeshko<sup>1\*</sup>, Olena Fesenko<sup>1</sup>, Andrej Dementjev<sup>2</sup>, Renata Karpicz<sup>2</sup>, Vladimir Fedorov<sup>3</sup> and Oleg Yu Posudievsky<sup>4</sup>

## Abstract

Coherent anti-Stokes Raman scattering (CARS) of carbon nanostructures, namely, highly oriented pyrolytic graphite, graphene nanoplatelets, graphene oxide, and multiwall carbon nanotubes as well CARS spectra of thymine (Thy) molecules adsorbed on graphene oxide were studied. The spectra of the samples were compared with spontaneous Raman scattering (RS) spectra. The CARS spectra of Thy adsorbed on graphene oxide are characterized by shifts of the main bands in comparison with RS. The CARS spectra of the initial nanocarbons are definitely different: for all investigated materials, there is a redistribution of D- and G-mode intensities, significant shift of their frequencies (more than  $20\text{ cm}^{-1}$ ), and appearance of new modes about  $1,400$  and  $1,500\text{ cm}^{-1}$ . The D band in CARS spectra is less changed than the G band; there is an absence of 2D-mode at  $2,600\text{ cm}^{-1}$  for graphene and appearance of intensive modes of the second order between  $2,400$  and  $3,000\text{ cm}^{-1}$ . Multiphonon processes in graphene under many photon excitations seem to be responsible for the features of the CARS spectra. We found an enhancement of the CARS signal from thymine adsorbed on graphene oxide with maximum enhancement factor about  $10^5$ . The probable mechanism of CARS enhancement is discussed.

**Keywords:** Graphene oxide (GO); Graphene nanoplatelets (GNPs); Multiwall carbon nanotubes (MWCNTs); Highly oriented pyrolytic graphite (HOPG); Thymine, Surface-enhanced Raman scattering (SERS); Coherent anti-Stokes Raman scattering (CARS); Surface-enhanced coherent anti-Stokes Raman scattering (SECARS); Graphene oxide-enhanced coherent anti-Stokes Raman scattering (GECARS)

## Background

Enhancement of optical signals (Raman scattering, infrared absorption (IR), and luminescence) from molecules adsorbed on the surface of nanostructured metals was considered in many papers published recently. The nanostructured gold, platinum, silver, copper, and other metals were used for the achievement of the enhancement effect. The enhancement factor could achieve  $10^6$  for Raman scattering and  $10^3$  for IR absorption and luminescence [1,2]. Moreover, surface-enhanced Raman scattering (SERS) effect allowed registration of the signal from a single molecule adsorbed on the nanostructured surface [3]. The mechanism of this effect possesses dual

electromagnetic (EM) and chemical (CM) nature and is the matter of debate in the literature [1-4].

Earlier, we have registered enhancement in Raman and IR spectra of different biomolecules adsorbed on carbon nanostructures: single-wall carbon nanotubes (SWCNTs) and graphene nanoflakes [5-7]. The maximum enhancement factor for Raman scattering of such nucleobases as thymine and adenine adsorbed on SWCNT was 10. It could be up to 80 on graphene oxide (GO) [8]. It is known from the literature that graphene could be used as enhancing support with enhancement factor from 17 to 69 [9-11].

The coherent anti-Stokes Raman scattering (CARS) technique is rather complex [12-14], and we found only a few papers devoted to its application for studying biomolecules [15-18]. The enhancement of CARS signal for molecules localized on nanostructured gold surface with

\* Correspondence: gd@iop.kiev.ua

<sup>1</sup>Institute of Physics, National Academy of Sciences of Ukraine, 46 Nauki Ave, Kyiv 03680, Ukraine

Full list of author information is available at the end of the article

an enhancement factor of approximately  $10^5$  was published in [17]. It was also established that this method is attractive for visualization of macromolecules and cell components [19].

In the present paper, we used CARS to study different carbon nanostructured materials (highly oriented pyrolytic graphite (HOPG), multiwall carbon nanotubes (MWCNTs), graphene nanoplatelets (GNPs), and GO) as well as the surface-enhanced coherent anti-Stokes Raman scattering (SECARS) effect for thymine (Thy) adsorbed on GO.

## Methods

### Samples

Thy was purchased from Sigma-Aldrich (St. Louis, MO, USA) and used as received. The MWCNTs (Spetsmash, Kiev, Ukraine) have been synthesized by CVD method using  $\text{Al}_2\text{FeMo}_{0.21}$  as a catalyst. The carbon content in the sample was 99.2% with soot as a residue; the catalyst was not found. The diameters of the MWCNTs varied from 2 to 40 nm; the surface area was  $350 \text{ m}^2/\text{g}$ . The material has been certified by high-resolution transmission electron microscopy and Raman scattering [20].

GO was synthesized from graphite using mechanochemical approach to exfoliate microflakes accordingly [21]. During the synthesis, sulfuric acid was added to the mixture of the graphite microflakes (#043480, Alfa Aesar, Ward Hill, MA, USA) and  $\text{KMnO}_4$  as an oxidant and then it was mechanochemically treated using a planetary ball mill. The product of the mechanochemical treatment was washed on a glass filter by distilled water to remove the residues of the reagents soluble in water and undesirable products of the oxidation reaction, then by aqueous hydrochloric acid to remove manganese oxides insoluble in water, which were formed as a result of reduction of  $\text{KMnO}_4$ , and finally with water to remove the residue of the acid. The product was placed in water where it quickly swelled and formed a stable dispersion of GO which was used thereafter. The prepared GO had C:H:O equal to 1.2:0.58:1.0 and an absorption maximum in UV-vis spectrum at 230 nm. It consisted of mono- and few-layered particles according to AFM and possessed photoluminescence with maximum of about 450 nm.

We used the GNPs produced by the Nikolaev Institute of Inorganic Chemistry, Siberian Branch of RAS (Novosibirsk, Russia). In accordance with the data of X-ray analysis and Raman spectroscopy, the GNPs predominantly consisted of 10 to 15 graphene layers with partial contribution of two- to three-layered nanoparticles. The lateral size of the GNPs was in the range from 5 to  $9 \mu\text{m}$  [22]. The graphene monolayer on Cu foil was purchased from Aldrich, and HOPG was produced by State Scientific Research Institute of Structural Graphite Based Materials 'NII Graphite' (Moscow, Russian Federation).

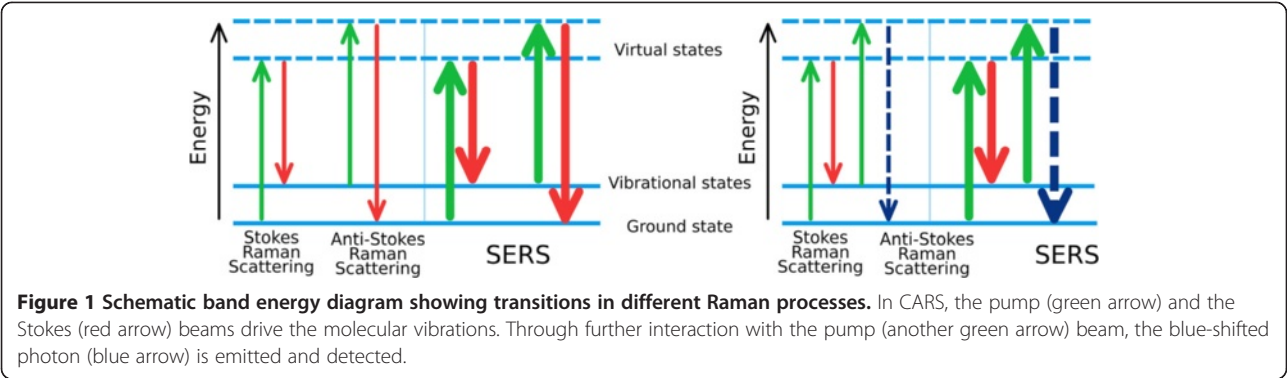
The stock aqueous solution of Thy (1 mg/ml) was first prepared and then divided into two aliquots. One part of the solution was taken for further experiments. Another part of the stock solution was ultrasonically mixed (15 min), with a definite amount of the GO to obtain Thy/GO = 100:1 weight ratio. The samples for further studies were prepared by depositing a drop of Thy or Thy/GO solution on a glass substrate for CARS and on a metallic surface for the Raman experiments.

### Raman measurements

The Raman spectra of the monolayer graphene on Cu and HOPG were registered by inVia Raman microscope (Renishaw, Wotton-under-Edge, UK) using a laser with 633-nm wavelength and spot size of  $1 \mu\text{m}$ . The Raman spectra of the MWCNTs, GO, and GNPs were also registered by inVia Raman microscope (Renishaw) using a diode laser with a wavelength of 785 nm. The SERS analysis of Thy/GO and Thy/MWCNT complexes was performed using the same laser. The band of Si at  $520 \text{ cm}^{-1}$  was used as the reference for wavenumber calibration. The WiRE 3.4 software (Renishaw) was used for Raman data acquisition and data analysis.

Carbon materials can be effectively characterized by Raman spectroscopy. The main feature of Raman spectra of graphite structure is the so-called 'G band' ( $1,600 \text{ cm}^{-1}$ ) with  $E_{1g}$  band symmetry [23] in the  $\Gamma$  point of the Brillouin zone that correlates with the ordering of graphite crystal lattice. The second feature of graphite-like materials is the so-called 'D band' that characterizes the disorder of graphene layer lattice [24]. It refers to breathing vibrations of rings of graphene layer in the K point of the Brillouin zone. The second-order mode of this vibration (2D band) is registered at 2,600 to  $2,700 \text{ cm}^{-1}$ , and it has an intensity which usually exceeds that of the second-order vibrations [25]. The last fact could be the evidence of carbon nanostructures consisting of similar structures that manifest a strong electron-phonon interaction and strong dispersion dependence of D-mode [24,25]. The characteristic feature of the Raman spectra of MWCNTs is that the halfwidth is equal to  $50 \text{ cm}^{-1}$  for the G-mode and above  $60 \text{ cm}^{-1}$  for the D-mode, and the D/G intensity ratio is greater than 1. The position of the G and D bands, appearance of breathing mode and its position, halfwidth, and relative intensity of all the bands could be used for the characterization of the nanotubes and their diameters.

The Raman spectrum of the graphene monolayer contains G and 2D bands analogous to graphite. The Raman spectrum of the GNPs and GO contains G, D, and 2D bands analogous to MWCNTs. The position of the 2D band maximum could be used as a characteristic to determine the number of layers in the graphene sheets [26].



**CARS measurements**

CARS phenomenon is based on nonlinear interaction of two incoming optical fields on frequency  $\omega_p$  (pump) and  $\omega_s$  (Stokes) with material, which results in the generation of blueshifted anti-Stokes light with frequency  $\omega_{AS} = 2\omega_p - \omega_s$ . Enhancement of the field on frequency  $\omega_{AS}$  takes place when the frequency difference  $2\omega_p - \omega_s$  coincides with the frequency of molecular vibrations of the studied material. Thus, tuning  $\omega_p$  while keeping  $\omega_s$  constant and detecting anti-Stokes light intensity, we could obtain CARS spectra containing information about the vibrational spectrum of the material. By spatial scanning the considered object at some fixed  $\omega_{AS}$ , we obtain a high-resolution image of the spatial distribution of the molecules possessing this particular vibrational band (Figure 1).

The experimental setup was described elsewhere [27]. Briefly, it is based on a home-made CARS microscope with compact laser source (EKSPLA Ltd., Vilnius, Lithuania). The laser consists of a picosecond (6 ps) frequency-doubled Nd:YVO<sub>4</sub> pump laser with a pulse repetition frequency of 1 MHz and equipped with a travelling wave optical parametric generator (OPG) with a turning range from 690 to 2,300 nm. For CARS implementation, the OPG radiation was coupled with a fundamental laser radiation (1,064 nm) used as pump and Stokes excitation beams, respectively. Such mixing provides probing within the 700 to 4,500 cm<sup>-1</sup> range of vibration frequencies. Both Stokes and pump beams were collinearly combined and directed to an inverted microscope (Olympus IX71, Center Valley, PA, USA). A spatial filter was used to improve the beam profile before directing into the microscope. The excitation light was focused on the sample with an oil immersion objective

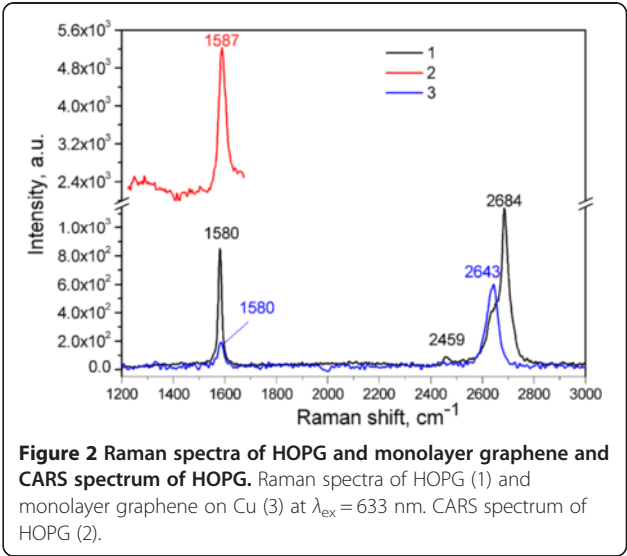
(Plan Apochromat, ×60, NA 1.42, Olympus). In the forward detection scheme, the CARS light was collected by another objective with NA 0.4. Long-pass and short-pass filters were used as blocking tools for spectral separation of the CARS signal. CARS radiation was detected using the avalanche photodiode (SPCM-AQRH-14, Perkin Elmer, Waltham, MA, USA) connected to a multifunctional board PCI 7833R (National Instruments Ltd. Dresden, Germany).

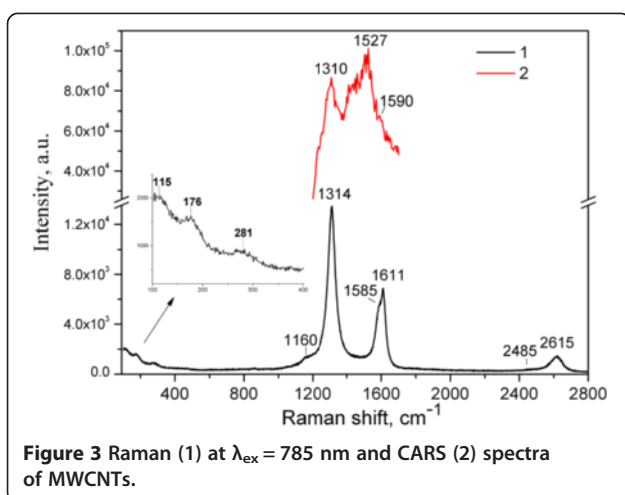
Measurements of the CARS spectra were performed in high-wavenumber region of Raman spectrum by tuning the OPG frequency (Table 1). In order to account for the spectral dependence of the OPG generation efficiency, the CARS signal intensity was normalized to the second power of the OPG radiation intensity. The spectral resolution of the CARS setup was approximately 8 cm<sup>-1</sup>. The spectra were recorded with a typical detection rate of 5 cm<sup>-1</sup>/s.

A Piezo scanning system (Physik Instrumente GmbH & Co., Karlsruhe, Germany) was used for scanning the samples. Images of 250 × 250 pixels were obtained with 2-ms pixel dwell time. Excitation pulse energies from 1

**Table 1** Operating CARS frequency

CARS registration range (cm <sup>-1</sup> )	Stokes (nm)	Pump (nm)	Anti-Stokes (or CARS) (nm)
1,200 to 1,700	1,064	940 to 900	850 to 780
2,500 to 3,500	1,064	840 to 775	690 to 610



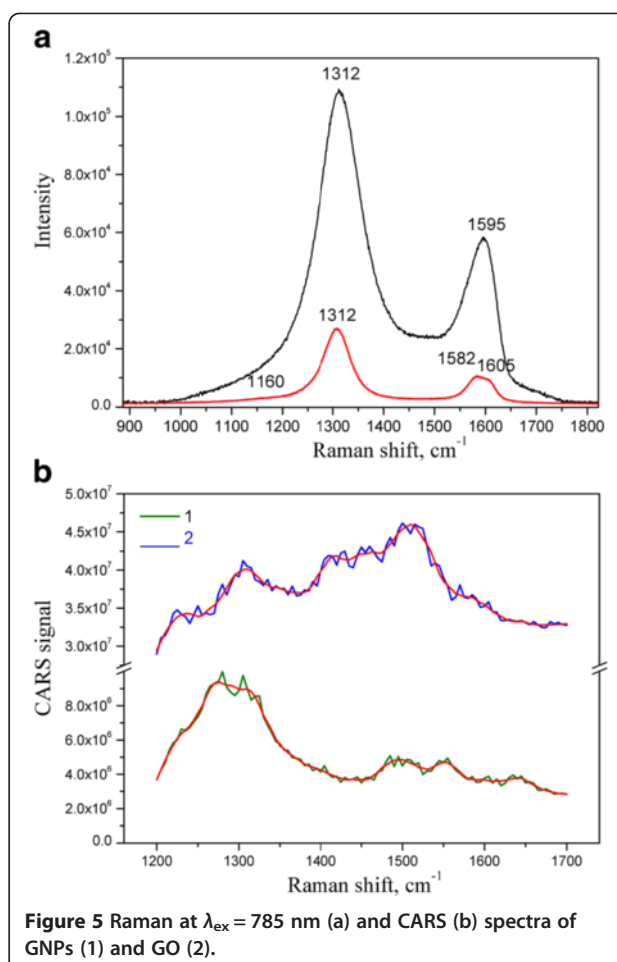


to 10 nJ of the samples for both pump and Stokes beams were used. Sample scanning, data processing, and laser wavelength tuning were controlled with a computer. The excitation light was focused on the sample with an oil immersion objective (Plan Apochromat,  $\times 60$ , NA 1.42, Olympus). This numerical aperture of the focusing objective provides tight focusing of NIR exciting light with effective lateral point spread function of about 0.4  $\mu\text{m}$ . The corresponding axial point spread function is about 1.0  $\mu\text{m}$ . Thus, the CARS images in this paper have resolutions of approximately 0.5  $\mu\text{m}$  in the  $X$  and  $Y$  directions, and approximately 1.0  $\mu\text{m}$  in the  $Z$  direction.

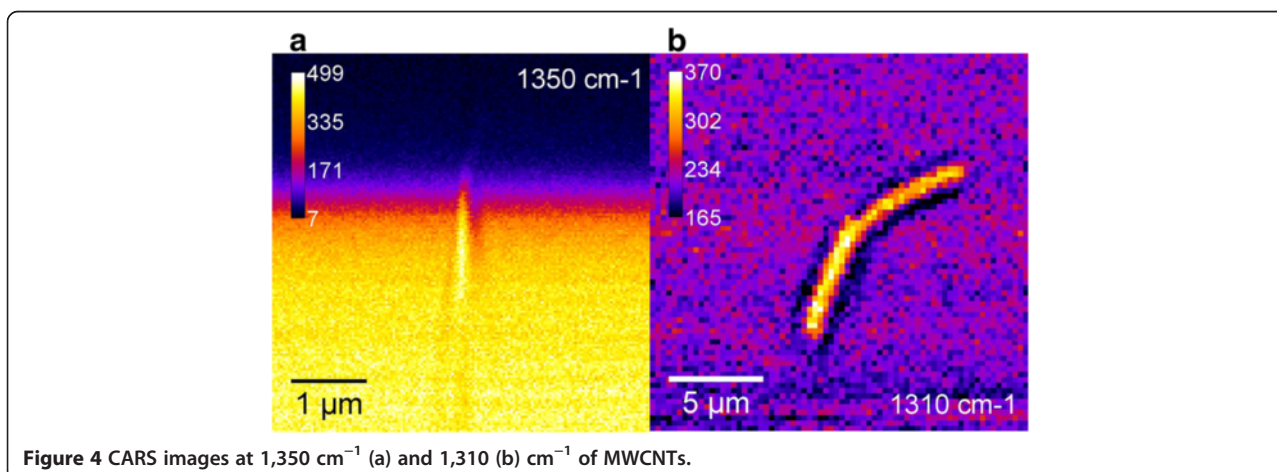
## Results and discussion

### Raman and CARS spectra of the carbon materials

The CARS and Raman spectra of the different carbon materials such as HOPG and monolayer graphene on Cu are presented in Figure 2 for comparison. The CARS spectra of the graphene monolayer on Cu foil could not be registered due to technical reasons; it was wrapped



and burned. It is seen that the position of the G-mode ( $1,580\text{ cm}^{-1}$ ) for HOPG and monolayer graphene is approximately the same with that in the Raman spectra. However, a definite high-frequency shift of  $7\text{ cm}^{-1}$  is observed for this mode in the CARS spectrum of HOPG.





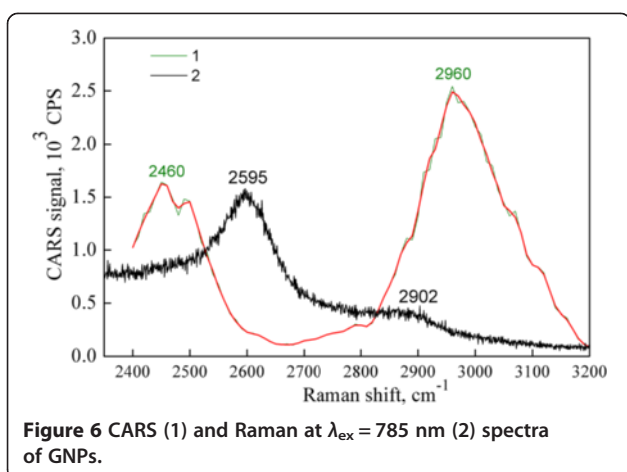


**Figure 6** CARS (1) and Raman at  $\lambda_{\text{ex}} = 785 \text{ nm}$  (2) spectra of GNPs.

The position of 2D-mode maximum in the Raman spectrum of HOPG is blueshifted by  $41 \text{ cm}^{-1}$  relatively to that of the monolayer graphene, the form of the band being asymmetric with a shoulder at approximately  $2,640 \text{ cm}^{-1}$ , a characteristic position of the band for the monolayer graphene.

The CARS and Raman spectra of MWCNTs are presented in Figure 3. The band in the Raman spectrum of MWCNTs about  $1,600 \text{ cm}^{-1}$  is asymmetric, consisting of G-mode at  $1,585 \text{ cm}^{-1}$  and D'-mode at  $1,611 \text{ cm}^{-1}$ . The G-mode in the CARS spectrum of MWCNTs is seen as a weak shoulder only (Figure 3) as compared with the strong new band at  $1,527 \text{ cm}^{-1}$  (denoted here as  $G_{\text{CARS}}$ ) and the shoulder at  $1,416 \text{ cm}^{-1}$ . In contrary to the Raman and CARS spectra of HOPG, the spectrum of MWCNTs contains D-mode which is indicative of the presence of defects. The Raman spectrum also contains several low-frequency modes (inset in Figure 3) whose positions could be used to determine the internal and external diameters of the nanotubes.

The images of the MWCNTs obtained using D-mode at  $1,310 \text{ cm}^{-1}$  are shown in Figure 4. Since CARS is a four-wave mixing (FWM) process, there are two contributions to the measured anti-Stokes signal: vibrational and electronic. The CARS spectrum of the MWCNTs has no distinct vibrational bands (Figure 3). That means that the contrast of the image has a predominantly electronic nature in accord with the earlier observations of the SWCNTs by FWM microscopy [28]. Moreover, in our case, the MWCNTs are located on the glass surface, and the scanning beam probes captured not only the MWCNTs but also the glass, so the contribution from the glass reduces the image contrast (Figure 4). Nevertheless, the lateral image recorded at the fixed value of  $z$  coordinate possesses a rather good contrast which allowed us to identify reliably the size of MWCNTs (Figure 4a,b). It appeared to be equal approximately to  $15 \mu\text{m}$  in length and approximately  $250 \text{ nm}$  in width. The image of the MWCNTs has the same intensity throughout the length which indicates a uniform distribution of defects.

The CARS and Raman spectra of the GNPs and GO are presented in Figure 5. It could be seen that the spectra are definitely different from each other for both carbon materials. For instance, the G-mode in the Raman spectrum of the GNPs is at  $1,582 \text{ cm}^{-1}$ , whereas in the CARS spectrum, it is shifted to  $1,555 \text{ cm}^{-1}$ . It is obviously strong and located at  $1,595 \text{ cm}^{-1}$  in the Raman spectrum of the GO, whereas it is about  $1,584 \text{ cm}^{-1}$  in the CARS spectrum in a form of a weak shoulder on the background of the strong band at  $1,516 \text{ cm}^{-1}$ . Analogously to the CARS spectrum of MWCNTs (Figure 3), the highly intensive  $G_{\text{CARS}}$ -mode at  $1,516 \text{ cm}^{-1}$  in the CARS spectrum of GO is observable. New arising bands at  $1,419$  and  $1,516 \text{ cm}^{-1}$  in GO and at  $1,500$  and  $1,555 \text{ cm}^{-1}$  in GNPs could be assigned to the vibrations from the edge atoms, and also

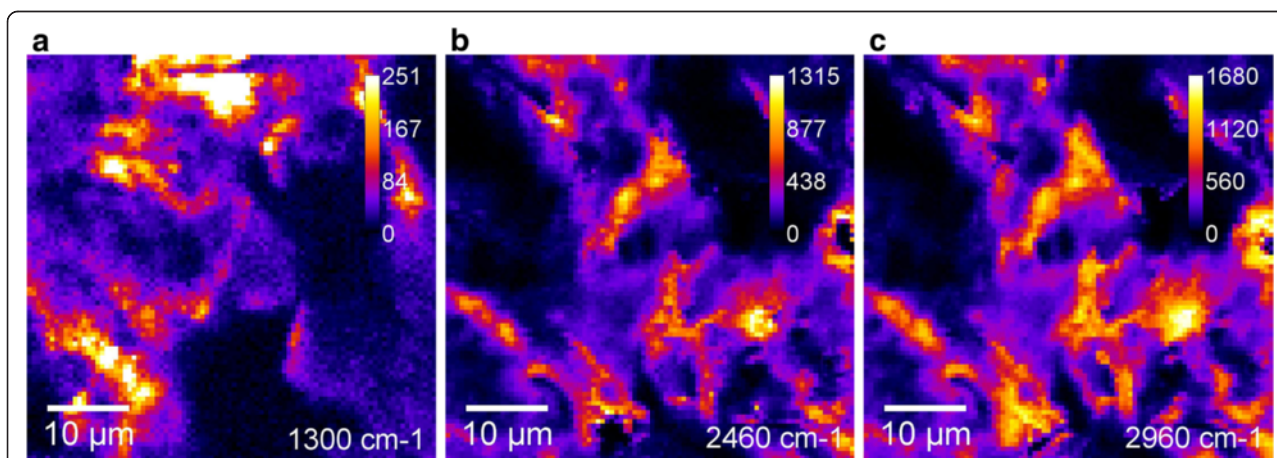


**Figure 7** CARS images of GNPs using the bands at  $1,300 \text{ cm}^{-1}$  (a),  $2,460 \text{ cm}^{-1}$  (b), and  $2,960 \text{ cm}^{-1}$  (c).

**Table 2 CARS bands of the different carbon materials**

Assignment	GNP (cm <sup>-1</sup> )	GO (cm <sup>-1</sup> )	MWCNT (cm <sup>-1</sup> )	HOPG (cm <sup>-1</sup> )
D	1,300	1,306	1,310	Not detected
New band	Not detected	1,419	1,421	Not detected
New band	1,500	1,516	1,527	Not detected
G	1,555	1,584	1,590	1,587
D'	Not detected	Not detected	Not measured	Not measured
2D (G')	Not detected	Not measured	Not measured	Not measured
D + D <sub>1</sub>	2,460	Not measured	Not measured	Not measured
2G <sub>CARS</sub>	2,960	Not measured	Not measured	Not measured

according to [14], the first principal calculation showed new emerging bands at 1,450 and 1,530 cm<sup>-1</sup>.

The position of D-mode in CARS and Raman spectra is approximately the same. Besides, it is worthwhile to mark the widening of the D-mode in the case of the CARS spectra of GNPs and the redistribution between  $I_D$  and  $I_G$  in the CARS spectra relatively to the Raman analogues.

Another feature of the interrelation between Raman and CARS spectra is observed in the 2,400 to 3,200 cm<sup>-1</sup> range. The corresponding spectra of the GNPs are presented in Figure 6. It is seen that the Raman spectrum of the GNPs has a usual form, as represented by the strong 2D-mode at 2,595 cm<sup>-1</sup>. At the same time, this mode is absent in the CARS spectrum, while there appeared another two strong band frequencies which are 2,460 and 2,960 cm<sup>-1</sup> (Figure 6). It could be supposed that the first is a combination of D-mode with a mode at approximately 1,150 cm<sup>-1</sup> (D<sub>1</sub>) which corresponds to a phonon belonging to a point other than K and  $\Gamma$  of the Brillouin zone [29], and the second is probably a double resonance of the 1,516 cm<sup>-1</sup> band. The disappearance of the 2D-mode is supposed to be connected with specificity of the CARS technique and the absence of the conditions for double electron-phonon resonance. Simultaneously, in the region of the second tones, we registered more bands than the usual, so multiphonon processes [30,31] could occur more efficiently.

The modes near 2,460 cm<sup>-1</sup> as well as those in the region of 2,400 to 3,200 cm<sup>-1</sup> are assigned to overtones [26]. Nemanich and Solin [24] have registered a band at 3,250 cm<sup>-1</sup> and a weaker band at 2,450 cm<sup>-1</sup> in the

Raman spectra of graphite. The last band was named as D'' by Vidano and Fishbach [25,32]. Later, Nemanich and Solin, using polarization measurement, assigned the peaks in the 2,300- to 3,250-cm<sup>-1</sup> region to overtones in graphite [24], and the 2,950-cm<sup>-1</sup> band to D + D' (D'-mode at 1,620 cm<sup>-1</sup> is due to disorder) rather than to D + G. Vidano and Fishbach [25] confirmed that

**Table 3 Raman bands of the different carbon materials**

Assignment	GNP (cm <sup>-1</sup> )	GO (cm <sup>-1</sup> )	MWCNT (cm <sup>-1</sup> )	HOPG (cm <sup>-1</sup> )
D-mode	1,307	1,312	1,314	Not detected
G-mode	1,582	1,595	1,589	1,580
D'	1,605	Not detected	1,611	Not detected
G'-mode (2D)	2,595	2,616	2,615	2,684
D + D' (or D + G)	2,902	Not detected	Not detected	Not detected

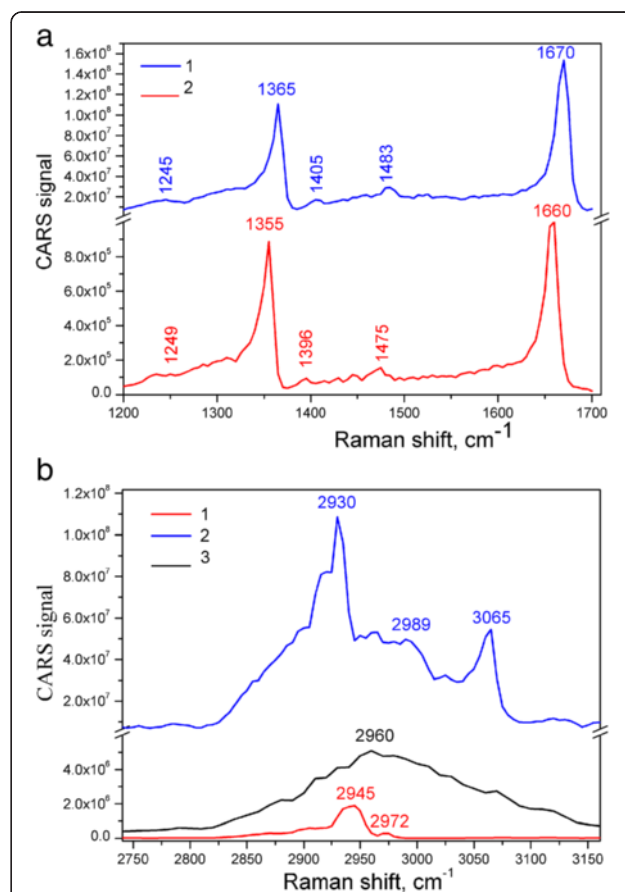


**Figure 8 CARS spectra of Thy/GO (1), Thy (2) and GNPs (3).** CARS spectra of Thy/GO (1) and Thy (2) in 1,200 to 1,700 cm<sup>-1</sup> (a) and CARS spectra of Thy/GO (1), Thy (2), and GNPs (3) in 2,400 to 3,200 cm<sup>-1</sup> (b) ranges.

the  $3,250\text{-cm}^{-1}$  band is the  $D'$  overtone, analogous to the band at  $2,700\text{ cm}^{-1}$  which is the  $D$  overtone named  $G'$ . Interestingly, those bands do not shift with excitation energy, and the energy dependence of the  $2,950\text{-cm}^{-1}$  band is consistent with  $D + D'$  or  $D + G$ .

The CARS images of the GNPs obtained using the different bands are presented in Figure 7. The distribution of the intensity of the CARS bands could be obviously seen: the intensities of the bands at  $2,460$  and  $2,960\text{ cm}^{-1}$  are similar, where the intensity of the signal at  $2,960\text{ cm}^{-1}$  is higher, so the image obtained using this band is brighter. Both the images and the spectrum of the GNPs have essentially vibrational origin. In accordance to [10] and Figure 7 (more bright imaging at the end of particles), we could suppose about the increase of the local electromagnetic field at the edges of the different graphene particles.

The modes found by using Raman and CARS spectroscopy in different carbon materials are summarized in Tables 2 and 3. Based on the presented data, it could be concluded that the position of the  $D$ -mode of the studied materials is close for Raman and CARS spectra; this is in contrary to that of the  $G$ -mode, which, in the CARS spectra, is significantly decreased on the background of the new intensive mode ( $G_{\text{CARS}}$ ), depending on the type of the carbon material.

#### Raman and CARS spectra of the Thy/GO complex

The CARS spectra of Thy and the Thy/GO complex are shown in Figure 8. It is seen that the bands of Thy

were shifted from  $1,355$  and  $1,660\text{ cm}^{-1}$  to  $1,365$  and  $1,670\text{ cm}^{-1}$  in Thy/GO complex, correspondingly. It could be suggested that these high-frequency shifts are due to the interaction of Thy with carboxyl and hydroxyl groups of GO [33]. The redistribution of the intensity of the bands and a new mode at  $3,065\text{ cm}^{-1}$  are characteristic of Thy/GO complex. Taking into account the presence of the wide band at  $2,960\text{ cm}^{-1}$  in the CARS spectrum of GNPs (Figure 6), it could be assumed that the widening of the CARS spectrum of Thy/GO complex is an evidence of the electron-phonon and phonon-phonon resonances [34]. The intensity of the CARS signals of the Thy/GO complex exceeds the CARS signals of Thy at more than  $10^4$  times.

The study of the Thy/GO complex by CARS spectroscopy was carried out in two spectral ranges. Both fingerprint and high-frequency ranges revealed strong bands belonging to Thy. The vibrational contribution to the spectra is dominating, so obtaining high-quality vibrational images of the complex is a possibility. The CARS images of Thy/GO recorded at several wavenumbers are shown in Figure 9. The bands at  $1,365$  and  $1,670\text{ cm}^{-1}$  and at  $2,930$ ,  $3,065$ , and  $3,300\text{ cm}^{-1}$  are used to obtain the images of two different fragments of the sample. Scans at  $2,930$ ,  $3,065$ , and  $3,300\text{ cm}^{-1}$  were done in  $50 \times 50\text{-}\mu\text{m}$  area and show the typical fragment entirely. All images have a very high contrast with respect to the image at  $3,300\text{ cm}^{-1}$ , where the background at non-resonance wavenumber is shown. It should be mentioned on the basis of comparison (Figure 9a,c) that the intensity of the CARS band at

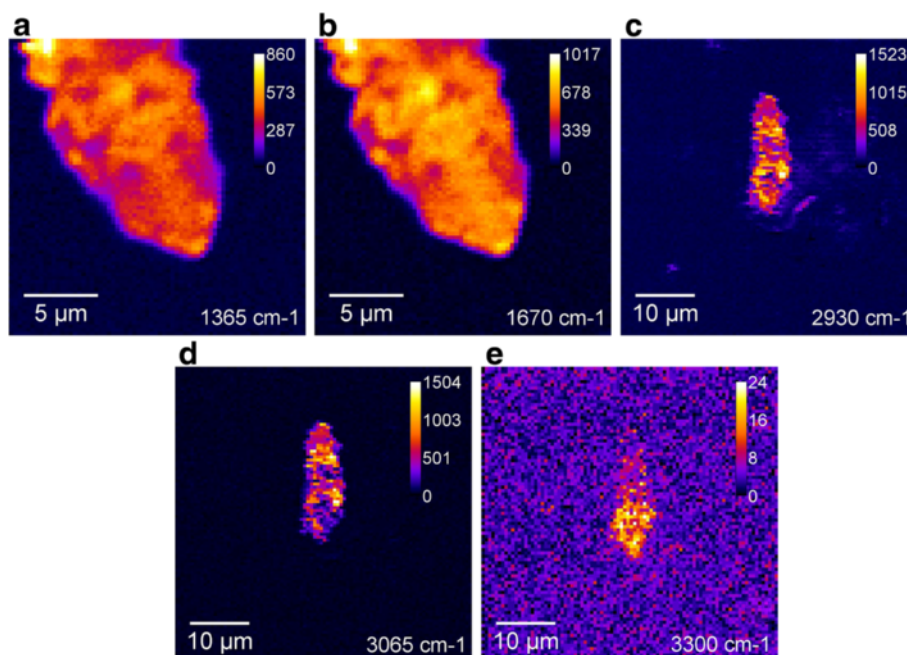


**Figure 9** CARS (a,b,c,d,e) images of the Thy/GO complex.

2,930  $\text{cm}^{-1}$  of Thy/GO is higher than that at 1,365  $\text{cm}^{-1}$  (one of the most intensive bands). This fact supports our assumption regarding the interaction between Thy and GO modes.

So, from the CARS images, it is seen that the Thy/GO complex adsorbed on the glass surface is not as a solid film but rather as flat flakes with lateral size from 1 to 15  $\mu\text{m}$ . It is important to note that the most intensive CARS bands of GNPs and Thy/GO are, respectively, at 2,960 and at 2,930  $\text{cm}^{-1}$ . So, it could be supposed that the enhancement of the CARS bands of the Thy/GO complex in the 2,930- to 3,100  $\text{cm}^{-1}$ -range is connected with the chemical interaction between Thy and GO.

The Raman spectra of Thy and the Thy/GO complex are shown in Figure 10. In the spectra of Thy/GO, the characteristic bands of GO (D-, G-, and 2D-modes) are clearly seen. Also, in the 2,750- to 3,200- $\text{cm}^{-1}$  range, the enhancement and widening of the characteristic bands

of Thy are observed. Importantly, these bands are the features of the CARS spectra as well (Figure 8).

The assignment of Raman and CARS spectral bands for Thy and Thy/GO complex is presented in Table 3. As a whole, the position of the bands in the Raman and CARS spectra is often close. In the CARS spectrum of the Thy/GO complex, there are NH and CH stretching modes in the 3,000- to 3,300- $\text{cm}^{-1}$  range, and the  $\text{C}_6\text{H}$  stretching modes of medium intensity are at 3,065  $\text{cm}^{-1}$ . It is interesting that in the CARS spectra of the Thy/GO complex (Table 4), there is only one band at 1,670  $\text{cm}^{-1}$ , whereas in the corresponding spectra of Thy, there are two bands at 1,655 and 1,660  $\text{cm}^{-1}$ , attributed to  $\text{C}_4\text{O}$  and  $\text{C}_2\text{O}$  stretching modes, respectively. A similar effect was observed in the case of SERS of Thy on gold in comparison with RS of those [35]; however, its nature could have another origin. It depends on the peculiarities of the CARS method and orientation of Thy in relation to graphene oxide surface.

To determine the enhancement factor of the CARS signal for the Thy/GO complex relative to Thy, the filling factor and the conditions of the CARS experiment

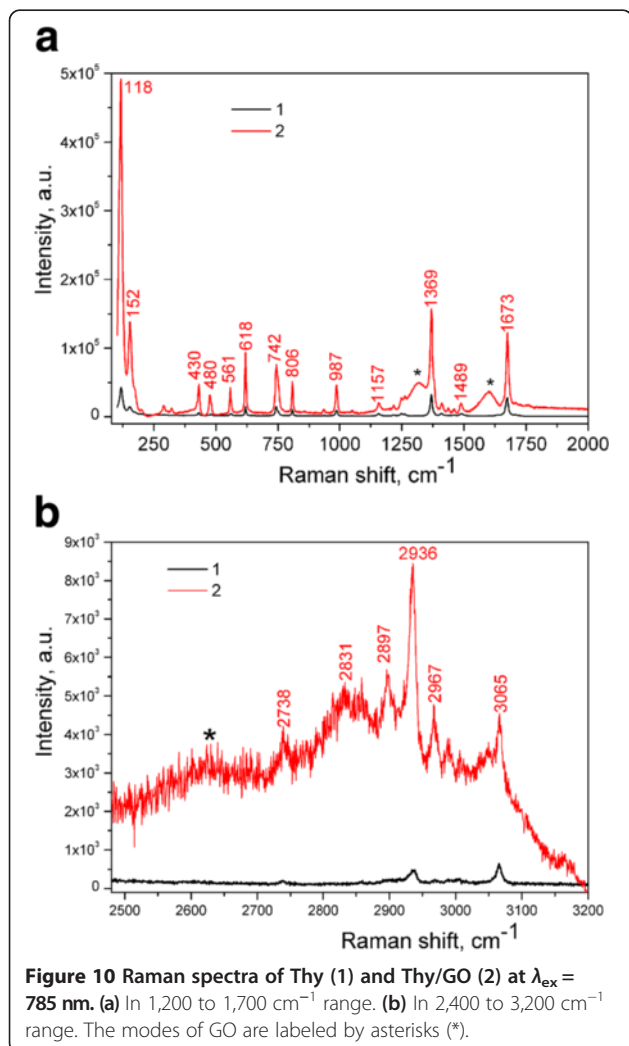


**Table 4** Assignment of the spectral bands ( $\text{cm}^{-1}$ ) observed for Thy and Thy/GO complex

RAMAN ( $\lambda_{\text{ex}} = 785 \text{ nm}$ ) spectra		CARS spectra		Assignment in Thy [36-38] and GO [33]
Thy	Thy/GO	Thy	Thy/GO	
-	-	-	3,300	$\nu$ (OH) in GO
-	-	-	3,167	$\nu$ (NH); $\nu$ (OH) GO
3,065	3,065	-	3,065	$\nu$ ( $\text{C}_6\text{H}$ )
3,006	3,005	-	2,991	$\nu$ ( $\text{CH}_3$ )
2,968	2,967	-	2,963	$\nu$ ( $\text{CH}_3$ )
2,989	2,989	2,972	2,989	$\nu$ ( $\text{CH}_3$ )
2,936	2,936	2,945	2,930	$\nu$ ( $\text{CH}_3$ )
2,892	2,897	2,870	-	$\nu$ ( $\text{CH}_3$ )
-	2,831	-	2,848	CH, GO
2,739	2,738	2,749	2,753	CH
-	2,626	-	-	2D-mode in GO
1,673	1,675	1,660	1,670	$\nu$ ( $\text{C}_2 = \text{O}$ )
-	-	1,655	-	$\nu$ ( $\text{C}_4 = \text{O}$ )
-	1,603	-	-	G-mode in GO
-	-	1,520	1,525	$\nu$ ring
1,489	1,490	1,482	1,483	$\delta\text{N}_1\text{H}$
1,460	1,459	1,461	1,458	$\delta_{\text{as}}$ ( $\text{CH}_3$ )
1,437	-	-	1,436	$\text{CH}_3$
1,411	1,410	1,406	1,405	$\nu\text{C}2\text{N}3$ , $\delta\text{N}_1\text{H}$
1,368	1,368	1,355	1,365	$\delta_s$ ( $\text{CH}_3$ ), $\delta$ ( $\text{N}_3\text{H}$ )
-	1,319	-	-	D-mode in GO
1,247	1,248	1,247	1,249	$\nu$ (ring)

$\nu$ , stretching;  $\delta$ , deformation. All bands are assigned to Thy; the bands assigned to graphene oxide are noted.



should be evaluated. In CARS experiments, the radiation comes from the space volume of approximately  $1\ \mu\text{m}^3$ . Such volume can contain approximately  $10^9$  molecules of Thy (without graphene). When GO is added to Thy, in accord with our estimation, the number of Thy molecules within the mentioned volume is approximately  $10^8$ . Then, taking into account these assumptions and the difference between the intensity of the CARS signal for the Thy/GO complex and Thy from Figure 8 (approximately  $10^4$ ), we could obtain that the CARS enhancement factor is equal to approximately  $10^5$ . The enhancement obviously arises from those molecules of Thy which are in close proximity to the surface of GO. The number of such Thy molecules is really lower than the whole number of the molecules in the volume. So, the obtained estimation of the enhancement factor should be considered as the lower limit. It could also be mentioned that the value of the enhancement factor is not the same for the whole range from 1,200 to  $3,300\ \text{cm}^{-1}$ . It is the maximum for the NH and CH stretching modes which usually appear in 3,000- to  $3,200\text{-cm}^{-1}$  range (Figure 8b).

The enhancement effect of the CARS spectrum of the Thy/GO complex seems to be similar to that of SECARS (Figure 8), and it could be named as graphene oxide-enhanced CARS (GECARS), analogous to the graphene-enhanced Raman scattering (GERS) technique, in which graphene can be used as a substrate for SERS of adsorbed molecules [9,11,39].

SERS enhancement is typically explained by CM [40] and EM [1,41-43] mechanisms. CM is based on charge transfer between the probed molecule and the substrate. On the other hand, the origin of EM mechanism is connected with great increase of the local electric field caused by plasmon resonance in nanosized metals, such as Ag and Au [41]. These two mechanisms always contribute simultaneously to the overall enhancement, and it is usually thought that EM provides the main enhancement. For graphene-type materials, due to the fact that surface plasmon in graphene is in terahertz range rather than within the range of visible light [44], GERS, in most cases, does not support the EM mechanism, and it is more appropriate to consider the CM. However, in the case of the GO, the oxygen-containing groups could create strong local electric field [45] under laser excitation, so large polarizability of graphene domains induces additional local electric field and increases the cross-section of RS of the adsorbed molecules. Additional enhancement could be explained by resonant excitation for one or two photons in the case of CARS of nanocarbons (Table 1) also. Indeed, our optical study in the near-visible range confirms the appearance of local density states of MWCNTs and GNPs in the region of 500 to 900 nm. So, resonant excitation could be the other

reason of giant enhancement in CARS. All this mechanisms need further study and analysis.

## Conclusions

Therefore, it was shown that the CARS spectra of carbon nanostructures (GNPs, GO, and MWCNTs) are definitely different from the corresponding spontaneous Raman spectra. At the same time, the CARS and Raman spectra of Thy are rather close and could be used for analytical purposes. The GECARS effect was shown for the Thy/GO complex with minor shifts of Thy bands. The enhancement factor of the GECARS signal for the Thy/GO complex is greater than approximately  $10^5$ . In our view, the enhancement effect could have several reasons: (a) the so-called chemical mechanism, which involves charge transfer between the molecule and the carbon nanostructure, as well as the increase of the dipole moment in the molecule; (b) the resonant interaction of exciting light with electronic states of the carbon nanostructures; and (c) the increase the local electromagnetic field at the edges of the GO nanosheets.

## Abbreviations

CARS: coherent anti-Stokes Raman scattering; CM: chemical mechanism; EM: electromagnetic mechanism; GECARS: graphene oxide-enhanced coherent anti-Stokes Raman scattering; GNP: graphene nanoplatelet; GO: graphene oxide; HOPG: highly oriented pyrolytic graphite; IR: infrared spectroscopy; MWCNT: multiwalled carbon nanotube; SERS: surface-enhanced Raman scattering; SECARS: surface-enhanced coherent anti-Stokes Raman scattering; SWCNT: single-walled carbon nanotubes.

## Competing interests

The authors declare that they have no competing interests.

## Authors' contributions

GD has given final approval of the version to be published. OF has made substantial contributions to the conception and design of the study and acquisition, analysis, and interpretation of data. AD has been involved in drafting the manuscript and in measuring the CARS spectra. RK has been involved in drafting the manuscript. VF carried out the synthesis of the graphene nanoplatelets. OP carried out the synthesis of graphene oxide and participated in drafting the manuscript. All authors read and approved the final manuscript.

## Authors' information

GD has a scientific degree of Doctor of Sciences in Solid State Physics and Biophysics and received degree of professor in 2012. She is a Head of Physics of the Biological Systems Department of Institute of Physics of National Academy of Sciences of Ukraine. Her scientific areas of interest are Biophysics, nucleic acids, Solid State Physics, surface solids, plasmonics, experimental physics (FTIR, SEIRA, SERS, UV, Raman, NMR spectroscopy, Langmuir-Blodgett technique, AFM microscopy, and Computational Chemistry). She was involved in the study of biological molecule interaction with low doses of ionizing and microwave irradiation, ligands, anti-cancer drugs, metal and carbon nanostructures. She has more than 250 publications in international scientific journals. OF received her degree of Senior Researcher in 2009 and her Ph.D. at Institute of Physics of National Academy of Sciences of Ukraine in 2007 with a thesis about effects and mechanisms of enhancement of optical transition of bio-organic molecules near metal surface. Now, she is the Head of the Innovations and Technology Transfer Department of the Institute of Physics of National Academy of Sciences of Ukraine. Her present study mainly focuses on the spectroscopical manifestation of SEIRA, SERS, enhanced luminescence effect of biological molecules, and development of metal enhancing supports for application. In 2009, her work 'The enhancement of the optical processes on the metallic surface and its application for the detection of small quantity

of molecules and revealing the structure of tumors macromolecules' was awarded with the Prize for Young Scientists from the President of Ukraine. She is currently managing FP7 Nanotwinning Project within the framework of which inVia Raman microscope (Renishaw) was purchased and is actively used in the experiments described in this article. OP is a Senior Research scientist in the Free Radicals Department of L.V. Pisarzhevsky Institute of Physical Chemistry of the National Academy of Science of Ukraine. He received his Ph.D. from L.V. Pisarzhevsky Institute of Physical Chemistry of the National Academy of Science of Ukraine in 1985. His research interests include preparation and physical chemistry of new functional materials, conducting polymers, graphene oxide, graphene and graphene-like nanomaterials, hybrid nanocomposites, sensors, lithium batteries, and light-emitting diodes. He is the author of more than 100 scientific publications. Also, he is a scientific referee of European FP6 and FP7, German-Israeli Foundation for Scientific Research and Development (GIF), numerous scientific journals published by Elsevier, Wiley, the Royal Society of Chemistry, and American Chemical Society. AD is a Ph.D. degree holder and a Senior Research Scientist in the Molecular Compounds Physics Department of State Research Institute Center for Physical Sciences and Technology. His main research interests include nonlinear optical microscopy, chemical imaging by means of coherent anti-Stokes Raman microscopy, application of coherent Raman microscopy to bio-objects, and optical nonlinearity of nanostructured organic polymers. He is a member of the management committee in COST Action 'Chemical Imaging by Coherent Raman Microscopy – microCoR' from Lithuania. RK works as a Senior Researcher in the Molecular Compound Physics Department at the Center for Physical Sciences and Technology. She defended her Ph.D. thesis in 2001 at the Institute of Physics, Vilnius. Her main research interests are spectroscopic characterization of organic materials, ultrafast excitation relaxation processes in organic molecular compounds, molecular isomerization, tautomerization, charge transfer processes, and charge carrier generation in organic semiconductors. She is the author of more than 25 scientific papers. VF received the following scientific degrees: Ph.D. in 1966, Doctor of Chemical Science in 1990 and the title of Full Professor in 1991. He was awarded with the title of Honored Science Worker of Russian Federation (2004). Currently, he works as the Chief Scientist at Nikolaev Institute of Inorganic Chemistry, Siberian Branch of Russian Academy of Sciences. He is a lecturer at the Natural Science Department of the Novosibirsk State University. He actively collaborates with universities in many countries. His research interests lie in the fields of solid state chemistry, synthesis and materials design, and crystal and electronic structures of low-dimensional inorganic materials with unusual electronic properties. He has more than 400 publications, including original articles, reviews, patents, and three books.

## Acknowledgements

We thank the FAEMCAR and ILSES Projects of Marie Curie Actions and Nanotwinning Project of FP7 Program for the financial assistance. Thanks as well to Dr. Yu. I. Sementsov (Kiev) and Prof. V. Levin (Moscow) for the samples of MWCNTs and HOPG, respectively, and A. Rynder for the measurement of the Raman spectra (Kiev).

## Author details

<sup>1</sup>Institute of Physics, National Academy of Sciences of Ukraine, 46 Nauki Ave, Kyiv 03680, Ukraine. <sup>2</sup>Institute of Physics, Center for Physical Sciences and Technology, A. Goštauto 11, Vilnius LT-01108, Lithuania. <sup>3</sup>Nikolaev Institute of Inorganic Chemistry, Siberian Branch of RAS, Akad. Lavrentiev Ave. 3, Novosibirsk 630090, Russia. <sup>4</sup>L.V. Pisarzhevsky Institute of Physical Chemistry, National Academy of Sciences of Ukraine, 31 Nauki Ave, 03028 Kyiv, Ukraine.

Received: 27 February 2014 Accepted: 16 April 2014

Published: 27 May 2014

## References

- Kosobukin V: The effect of enhancement the external field near the surface of metal and its manifestation in spectroscopy. *Surface: Phys Chem Mech* 1983, **12**:5–20.
- Domingo C: Infrared spectroscopy on nanosurfaces. *Opt Pur Apl* 2004, **16**:567–571.
- Le Ru EC, Etchegoin PG: Single-molecule surface-enhanced Raman spectroscopy. *Annu Rev Phys Chem* 2012, **63**:65–87.
- Wang X, Shi W, She G, Mu L: Surface-enhanced Raman scattering (SERS) on transition metal and semiconductor nanostructures. *Phys Chem Chem Phys* 2012, **14**:5891–5901.
- Dovbeshko G, Fesenko O, Gnatyuk O, Yakovkin K, Shuba M, Maksimenko S: Enhancement of the infrared absorption by biomolecules adsorbed on single-wall carbon nanotubes. In *Physics, Chemistry and Application of Nanostructure*. Edited by Borisenko V. London: World Scientific; 2011:291.
- Dovbeshko G, Fesenko O, Rynder A, Posudievsky O: Enhancement of infrared absorption of biomolecules adsorbed on single-wall carbon nanotubes and graphene nanosheets. *J Nanophotonics* 2012, **6**:061711.
- Dovbeshko G, Fesenko O, Gnatyuk O, Rynder A, Posudievsky O: Comparative analysis of the IR signal enhancement of biomolecules adsorbed on graphene and graphene oxide nanosheets. In *Nanomaterials Imaging Techniques, Surface Studies, and Applications*. Edited by Fesenko O, Yatsenko L, Brodyn M. Dordrecht: Springer; 2013:1–10.
- Rinder A, Dovbeshko G, Fesenko O, Posudievsky O: Surface-enhanced Raman scattering of biomolecules on graphene layers [abstract]. In *Nanotechnology: from Fundamental Research to Innovations*. Edited by Yatsenko L, Bukovel: EvroSvit; 2013:s55.
- Xi L, Xie L, Fang Y, Xu H, Zhang H, Kong J, Dresselhaus M, Zhang J, Liu Z: Can graphene be used as substrate for Raman enhancement? *Nano Lett* 2010, **10**:553–561.
- Huang C, Kim M, Wong BM, Safran NS, Arnold MS, Gopalan P: Raman enhancement of a dipolar molecule on graphene. *J Phys Chem* 2014, **118**:2077–2084.
- Xu W, Mao N, Zhang J: Graphene: a platform for surface-enhanced Raman spectroscopy. *Nano Micro Small* 2013, **8**(9):1206–1224.
- Kima H, Sheps T, Taggart D, Collinsb P, Pennera R, Potmaa E: Coherent anti-Stokes generation from single nanostructures. *Proc of SPIE* 2009, **7183**:718312-1.
- Chen CK, De CAHB, Shen YR, De Martini F: Surface coherent anti-Stokes Raman spectroscopy. *Phys Rev Lett* 1979, **43**:946–949.
- Day JPR, Domke KF, Rago G, Kano H, Hamaguchi H, Vartiainen EM, Bonn M: Quantitative coherent anti-Stokes Raman scattering (CARS) microscopy. *J Phys Chem B* 2011, **115**:7713–7725.
- Baltog I, Baibarac M, Lefrant S: Coherent anti-Stokes Raman scattering on single-walled carbon nanotube thin films excited through surface plasmons. *Phys Rev B* 2005, **72**:245402.
- Song B, Cuniberti G, Sanvito S, Fang H: Nucleobase adsorbed at graphene devices: enhance bio-sensors. *Appl Phys Lett* 2012, **100**:063101.
- Steuwe C, Kaminski C, Baumberg J, Mahajan S: Surface enhanced coherent anti-Stokes Raman scattering on nanostructured gold surfaces. *Nano Lett* 2011, **12**:5339–5343.
- Segawa H, Okuno M, Kano H, Leproux P, Couderc V, Hamaguchi H: Label-free tetra-modal molecular imaging of living cells with CARS, SHG, THG and TSFG (coherent anti-Stokes Raman scattering, second harmonic generation, third harmonic generation and third-order sum frequency generation). *Opt Express* 2012, **9**:9551–9557.
- Rago G, Langer C, Brackman C, Day JPR, Domke KF, Raschzok N, Schmidt C, Sauer IM, Enejder A, Mog MT, Bonn M: CARS microscopy for the visualization of micrometer-sized iron oxide MRI contrast agents in living cells. *Biomed Optics Expr* 2011, **2**:2472–2483.
- Melezhuk A, Yanchenko V, Sementsov Y: Nanocarbon materials. In *Hydrogen Materials Science and Chemistry of Carbon Nanomaterials*. Edited by Veziroglu TN, Zaginichenko SY, Schur DV, Baranowski B, Shpak AP, Skorokhod W, Kale A. New York: Springer; 2007:529-237.
- Posudievsky OY, Kozarenko OA, Khazieva OA, Koshechko VG, Pokhodenko VD: Ultrasound-free preparation of graphene oxide from mechanochemically oxidized graphite. *J Mater Chem A* 2013, **1**:6658–6663.
- Grayfer E, Makotchenko V, Nazarov A, Kim S, Fedorov V: Graphene: chemical approaches to synthesis and modification. *Rus Chem Rev* 2011, **80**:784–804.
- Bir GL, Pikus GE: *Symmetry and Deformation Effects in Semiconductors*. Moscow: Nauka; 1972:584.
- Nemanich R, Solin S: First- and second-order Raman scattering from finite-size crystals of graphite. *Phys Rev B* 12 1979, **20**:392.
- Vidano R, Fishbach D: Observation of Raman band shifting with excitation wavelength for carbons and graphites. *Solid State Comm* 1981, **39**(2):341–344.
- Ferrari A, Basko D: Raman spectroscopy as a versatile tool for studying the properties of graphene. *Nat Nanotechnol* 2013, **8**:235–246.

27. Dementjev A, Gulbinas V, Serbenta A, Kaucikas M, Niaura G: **Coherent anti-Stokes Raman scattering spectroscopy/microscope based on a widely tunable laser source.** *J Modern Optics* 2010, **57**(6):503–509.
28. Kim H, Sheps T, Collins P, Potma E: **Nonlinear optical imaging of individual carbon nanotubes with four-wave-mixing microscopy.** *Nano Lett* 2009, **8**:2991–2995.
29. Strelchuk VV, Nikolenko AS, Gubanov VO, Biliy MM, Bulavin LA: **Dispersion of electron-phonon resonances in one-layer graphene and its demonstration in micro-Raman scattering.** *J Nanosci Nanotechnol* 2012, **12**:8671–8675.
30. Lui C, Malard LM, Kim S, Lantz G, Laverge FE, Saito R, Heinz TF: **Observation of layer-breathing mode vibrations in few-layer graphene through combination Raman scattering.** *Nano Lett* 2012, **12**:5539–5544.
31. Popov VN, Lambin P: **Theoretical polarization dependence of the two-phonon double-resonant Raman spectra of graphene.** *Eur Phys J B* 2012, **85**:418–426.
32. Vidano R, Fischbach DB: **New bands in the Raman spectra of carbons and graphite.** *J Am Ceram Soc* 1978, **61**:13–17.
33. Acik M, Lee G, Mattevi C, Chhowalla M, Cho K, Chabal Y: **Unusual infrared-absorption mechanism in thermally reduced graphene oxide.** *Nat Mater* 2010, **9**:840–845.
34. Yuratic MA, Hanna DC: **Coherent anti-Stokes Raman spectroscopy (CARS): selection rules, depolarization ratios and rotational structure.** *Mol Phys* 1977, **33**(3):671–682.
35. Otto C, Tweel TJJ, De Mul FFM, Greve J: **Surface-enhanced Raman spectroscopy of DNA bases.** *J Raman Spectrosc* 1986, **17**:289–298.
36. Singh J: **FTIR and Raman spectra and fundamental frequencies of biomolecule: 5-methyluracil (thymine).** *J Mol Struct* 2008, **876**:127–133.
37. Colarusso P, Benkrid K, Rode S, Midoux N, KeQing Z, Bujin G, Bernath PF: **The infrared spectra of uracil, thymine, and adenine in the gas phase.** *Chem Phys Lett* 1997, **269**:39–48.
38. Aroca R, Bujalski R: **Surface enhanced vibrational spectra of thymine.** *Vib Spectrosc* 1999, **19**:11–21.
39. Dovbeshko G, Fesenko O, Dementjev A: **Graphene enhanced Coherent anti-Stokes Raman spectroscopy [abstract].** In *Applied use of surface enhanced and laser spectroscopy*. Edited by Dolgov L. Estonia. University of Tartu; 2014:11.
40. Kambhampati P, Child CM, Foster MC, Campion AJ: **On the chemical mechanism of surface enhanced Raman scattering: experiment and theory.** *Chem Phys* 1998, **108**:5013–5026.
41. Osawa M: **Surface-enhanced infrared absorption spectroscopy.** In *Handbook of Vibrational Spectroscopy*. 1st edition. Edited by Chalmers JM, Griffiths PR. Chichester: Wiley; 2002:85–799.
42. Emelyanov VI, Koroteev NI: **The effect of Raman scattering by molecules adsorbed on the metal surface.** *Physics-Uspekhi* 1981, **135**(2):345–361.
43. Garrell RL: **Surface-enhanced Raman spectroscopy.** *Anal Chem* 1989, **61**:401A–411A.
44. Rana F: **Graphene terahertz plasmon oscillators.** *IEEE Trans Nanotechnol* 2008, **7**:91–99.
45. Lopes M, Candini A, Urdampilleta M, Reserbat-Plantey A, Bellini V, Klyatskaya S, Marty L, Ruben M, Affronte M, Wernsdorfer W, Bendjab N: **Surface-enhanced Raman signal for terbium single-molecule magnets grafted on graphene.** *ACS Nano* 2010, **4**(12):127531–127537.

doi:10.1186/1556-276X-9-263

**Cite this article as:** Dovbeshko et al.: Coherent anti-Stokes Raman scattering enhancement of thymine adsorbed on graphene oxide. *Nanoscale Research Letters* 2014 **9**:263.

**Submit your manuscript to a SpringerOpen<sup>®</sup> journal and benefit from:**

- Convenient online submission
- Rigorous peer review
- Immediate publication on acceptance
- Open access: articles freely available online
- High visibility within the field
- Retaining the copyright to your article

---

Submit your next manuscript at ► [springeropen.com](http://springeropen.com)